Complex Voltage-Dependent Behavior of Single Unliganded Calcium-Sensitive Potassium Channels

Gargi Talukder and Richard W. Aldrich
Department of Molecular and Cellular Physiology, Howard Hughes Medical Institute, Stanford University School of Medicine, Stanford, California 94305 USA

ABSTRACT The study and characterization of unliganded openings is of central significance for the elucidation of gating mechanisms for allosteric ligand-gated ion channels. Unliganded openings have been reported for many channel types, but their low open probability can make it difficult to study their kinetics in detail. Because the large conductance calcium-activated potassium channel *mSlo* is sensitive to both intracellular calcium and to membrane potential, we have been able to obtain stable unliganded single-channel recordings of *mSlo* with relatively high opening probability. We have found that the single-channel gating behavior of *mSlo* is complex, with multiple open and closed states, even when no ligand is present. Our results rule out a Monod–Wyman–Changeux allosteric mechanism with a central voltage-dependent concerted step, and they support the existence of quaternary states with less than the full number of voltage sensors activated, as has been suggested by previous work involving measurements of gating currents.

INTRODUCTION

Ion channels are transmembrane proteins that transduce appropriate stimuli into selective ion movement across the cell membrane. The basic characteristic of most channels' gating is of rapid transitions between two fixed primary conducting conformations, open and closed, whose probability of occurrence is influenced by gating stimuli such as ligand binding or voltage sensor movement. Channel gating is a compelling example of an allosteric mechanism, in that the gating stimulus, such as ligand binding, occurs at a site remote from the ion-conducting pore and influences transitions between two functional conformational states (Changeux and Edelstein, 1998; Edelstein and Changeux, 1996, 1998). In multimeric proteins, allosteric regulation is closely related to cooperativity between the subunits of the multimer. Cooperative subunit interactions mediated by allosteric influences between subunits can be important for generating steep nonlinear stimulus–response relationships (see, for instance Fersht, 1985). A central question in understanding the gating of ion channels and other allosteric proteins is the relative roles of intrasubunit conformational changes and intersubunit cooperative interactions.

Large conductance calcium-sensitive potassium channels (BK channels) serve as a useful model system for the study of allosteric conformational changes. Their dual sensitivity to calcium binding and to membrane voltage, along with their homotetrameric structure, provides a wealth of allosteric phenomenology amenable to a wide range of experimental manipulations. In addition, their large single-channel conductance makes them ideal for single-molecule studies of conformational changes with submillisecond time resolution, a property that has been extensively exploited in studies of gating kinetics in the presence of calcium (Silberberg et al., 1996; Blatz and Magleby, 1983; Magleby and Pallotta, 1983a,b; McManus and Magleby, 1988, 1989, 1991; Neyton, 1996; Pallotta et al., 1981, 1992;Rothberg et al., 1996; Rothberg and Magleby, 1998; Methfessel and Boheim, 1982; Moczydlowski and Latorre, 1983; Rothberg and Magleby, 1999).

A central question in the study of allosteric ligand binding proteins has been the issue of whether ligand binding induces an allosteric conformational change, typified by the Koshland–Nemethy–Filmer (KNF) model (Koshland et al., 1966) developed for hemoglobin (Fig. 1 *A*), or whether it influences a pre-existing equilibrium between resting and active conformations, typified by the Monod–Wyman–Changeux (MWC) model (Monod et al., 1965) (Fig. 1 *B*). A requirement of the MWC class of models is that the unliganded protein is able to adopt the activated conformation. Conversely, KNF-type models require that the protein first bind a ligand before it can move to the activated state (Koshland et al., 1966). In the case of ion channels, the MWC model predicts that the channel can open even with no ligand bound (see Fig. 1 *B*, *boxed region*). Such unliganded openings have been reported for a variety of channels, such as calcium-activated potassium channels (Pallotta, 1985), cyclic nucleotide-gated channels (Picones and Korenbrot, 1995; Ruiz and Karpen, 1997; Tibbs et al., 1997), and acetylcholine receptors (Brehm et al., 1984; Jackson, 1984). However, detailed kinetic studies of unliganded openings are difficult for these channels because their probability of being open is very low (for example, $= 1.25 \times 10^{-4}$ (Tibbs et al., 1997) when ligand is not bound to the protein.

Although previous studies of single BK channels have involved sophisticated analyses of gating behavior, they

Received for publication 24 August 1999 and in final form 10 November 1999.

Address reprint requests to Richard W. Aldrich, Department of Molecular and Cellular Physiology, Howard Hughes Medical Institute, Stanford University School of Medicine, Stanford, CA 94305. Tel.: 650-723-6531; Fax: 650-725-4463; E-mail: raldrich@leland.stanford.edu.

0006-3495/00/02/761/12 $2.00

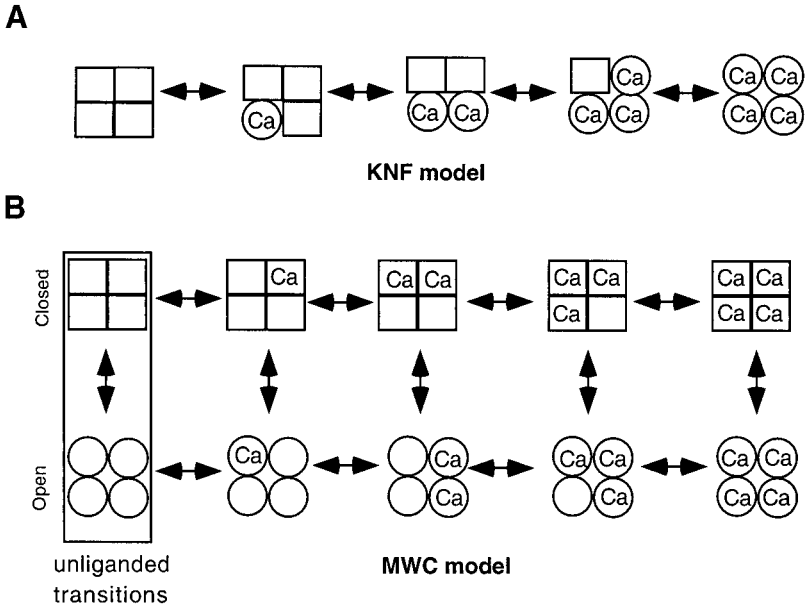

FIGURE 1 Two models commonly used to describe the functional properties of allosteric proteins are the (A) Koshland–Nemethy–Filmer (KNF) model and the (*B*) Monod–Wyman–Changeux (MWC) model. The models are pictured with calcium as a representative ligand. One particular difference between the two models is that, unlike the KNF model, the MWC model requires that the unliganded molecule is able to make the transition from the resting to the activated conformational state.

were, with few exceptions, conducted in the presence of calcium and did not account for the possibility of unliganded openings. However, it has been shown that, even in the absence of calcium, macroscopic BK currents can be nearly maximally activated by strongly positive voltage steps (Cui et al., 1997; Cox et al., 1997 Horrigan et al., 1999; Stefani et al., 1997).

Investigation of the macroscopic kinetics of the cloned BK channel *mSlo* has led to a proposed model of channel gating analogous to the allosteric MWC model (Cox et al., 1997). This voltage-dependent MWC model (see Fig. 1 *B*) has open and closed states corresponding to different numbers of calcium ions bound (0–4), with a single voltage-dependent allosteric transition between each closed state and its adjacent open state. A key difference between this model and models derived from previous studies of BK channel gating is that the MWC-like model accounts for opening of the unliganded channel through the channel's ability to respond to changes in membrane voltage. In the voltage-dependent MWC scheme, the unliganded channel exists in one of only two possible conformational states: open or closed (Fig. 1, *boxed region*). However, recent work on macroscopic ionic and gating currents suggests that the intrinsically voltage-dependent behavior of unliganded *mSlo* channels is more complex than the two-state mechanism predicted by this version of the voltage-dependent MWC model (Horrigan and Aldrich, 1999; Horrigan et al., 1999).

We have taken advantage of *mSlo*'s voltage sensitivity to study the gating of single unliganded *mSlo* channels. Our goal was to determine whether the complexity seen in previous studies of liganded BK channels remains in the gating of the unliganded channel, or if the unliganded channel is only able to gate with a single concerted transition between the open and closed state of the channel, as suggested by the voltage-dependent MWC model of Cox et al. (1997). We have approached this question at the single-channel level to ensure that any complexity we see in channel gating is due to the actions of a single molecule, and is not an apparent complexity that could arise from a heterogeneous population of channels in a macropatch. Regardless of the details of a particular model for BK channel gating, only a subset of the total available kinetic states are available when no calcium is bound to the channel, allowing study of the channel's gating within a subset of its total mechanism.

MATERIALS AND METHODS

All experiments were performed with the mbr5 clone of the mouse homolog of the *slo* gene (*mSlo*), which was kindly provided to us by Dr. Larry Salkoff (Washington University School of Medicine, St. Louis, MO). The cDNA was propagated in a modified Blue Script vector BS-MXT (Stratagene Inc., La Jolla, CA) in the *E. coli* strain DH5-α. cRNA was transcribed from this vector in vitro using the mMessage mMachine kit with T3 polymerase (Ambion In., Austin TX). ~0.005 ng of cRNA were injected into *Xenopus laevis* oocytes 2–3 days before recording.

All recordings were conducted in the inside-out patch clamp configuration at room temperature. Patch pipettes were made of borosilicate glass (VWR Micropipettes, West Chester, PA). Their tips were coated with wax (Kerr Corp, Romulus, MI) and fire polished before use. Data were acquired using an Axopatch 200-A patch clamp amplifier (Axon Instruments, Foster City, CA) in the resistive feedback mode and a Macintosh based computer system using Pulse acquisition software (HEKA Electronik, Lambrecht, Germany) with an ITC-16 hardware interface (Instrutech Scientific Instruments, Great Neck, NY). Records were digitized at 20-μs intervals and low pass filtered at 8 kHz.

Recording solutions were composed of the following (in mM): External (pipette): 140 $KMeSo_3$, 20 HEPES, 2 KCl, $2MgCl_2$ (pH = 7.20). Internal: 140 $KMeSo_3$, 20 HEPES, 2 KCl, 1 HEDTA and $CaCl_2$ to give the appropriate free Ca^{2+} concentration. For zero calcium solutions, 5 mM

EGTA was included (calculated free calcium = 0.5 nM). All internal solutions also included 40 μM (+)-18-crown-6-tetracarboxylic acid to chelate any contaminant barium (Diaz et al., 1996; Neyton, 1996). Solutions were exchanged at the cytoplasmic face of the patch using a sewer-pipe flow system (DAD 12, Adams and List Assoc. Ltd., Westbury, NY).

Data were analyzed using the ScanApp analysis program developed in the laboratory by Dorothy Perkins and Dan Cox. Sums of exponentials were fit directly to the dwell time data using the maximum likelihood method (Colquhoun and Sigworth, 1995). The appropriate number of exponentials were determined using the log-likelihood ratio test (Horn and Lange, 1983; Rao, 1973). To minimize errors due to filter cutoff, events shorter than 50 μs were not included in the fitting routine (Blatz and Magleby, 1986).

For the analysis of burst and interburst durations, a burst criterion of ~1 ms was determined from the data using the method of Colquhoun and Sakmann (1985).

RESULTS

Because strongly positive voltages (=120 mV) are required to open *mSlo* channels in the absence of calcium, we used repetitive steps to the indicated test voltage (Fig. 2), rather than the continuous recordings more commonly seen in previous analyses of single BK channel gating. The patches were better able to withstand the necessary voltages if the steps were kept relatively short (25 ms). Using voltage steps also allowed us to construct ensemble averages to compare with macroscopic current behavior.

Figure 2 displays traces from a single patch in the virtual absence of calcium, as well as a control set of traces recorded in the presence of 10 μM calcium. It was straightforward to identify single *mSlo* channels due to their large conductance (=250 pS) and the sensitivity of their apparent P_o to internal calcium (see the left most column of traces in Fig. 2). These data are representative of five single-channel patches studied at multiple voltages in the absence of calcium.

A two-state concerted open-to-closed behavior predicted by the voltage-dependent MWC model in Fig. 1 *B* is supported by the near single exponential kinetics of macroscopic current activation (Cui et al., 1997; Cox et al., 1999, however see Horrigan et al., 1999). To compare the average single-channel gating behavior to macroscopic currents, we constructed ensemble averages of hundreds of sweeps at various voltages in zero calcium (Fig. 2, *bottom row*). Like the macroscopic currents, the ensemble averages can be described by single-exponential kinetics, consistent with the idea of a single concerted allosteric transition. The time constants of single-exponential fits to the ensemble averages are similar to macroscopic current time constants (Fig. 3 *A*) above +200 mV, indicating that the average kinetics of the single-channel data are similar to what has been reported for macroscopic current behavior (Cui et al., 1997). At voltages lower than +200 mV, the ensemble averages seem to activate more slowly than macroscopic currents. How-

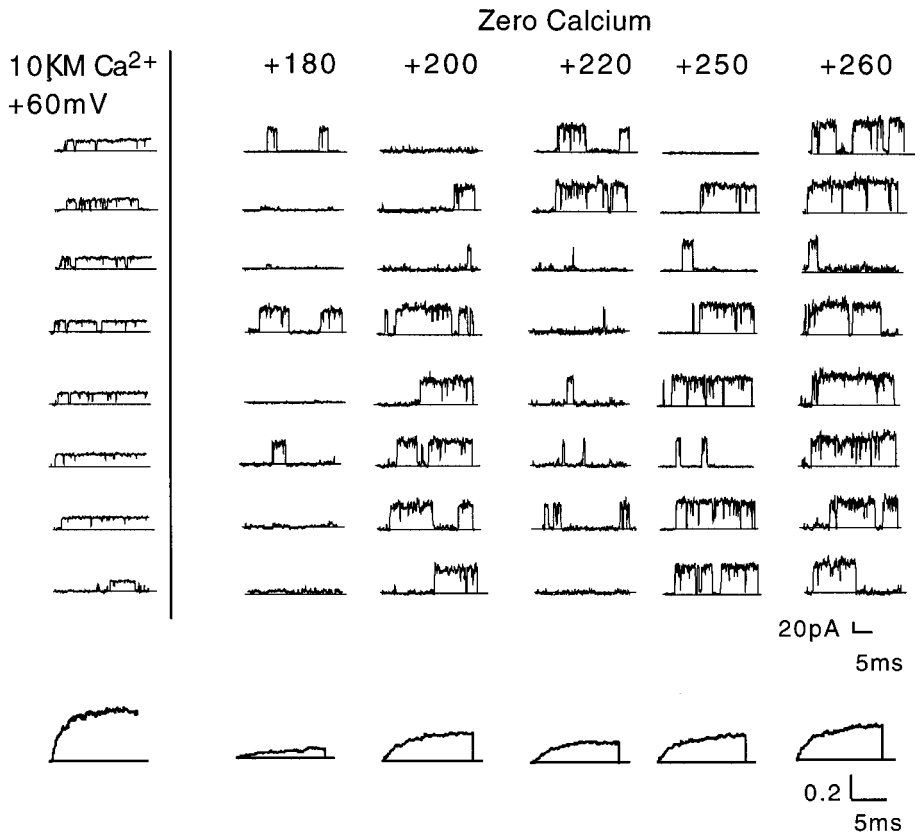

FIGURE 2 Representative single-channel records from a single patch across a range of voltages. The leftmost column of traces were recorded in 10 μM internal calcium to show that the behavior of these channels is qualitatively similar to what has been reported previously (see Pallotta et al., 1981). All other traces were recorded in 5 mM EGTA, zero added calcium. Ensemble averages for each voltage are pictured in the bottom row. 150–400 sweeps went into each of the ensemble averages.

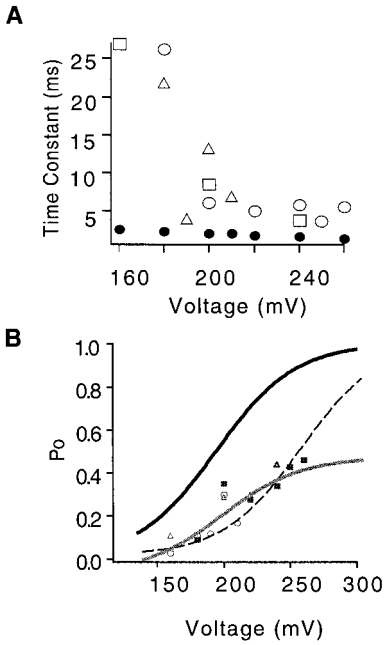

FIGURE 3 Single channel behavior in zero internal calcium is similar to previously described macroscopic current behavior. (*A*) The time constants of single exponential fits to the ensemble averages from three different patches are plotted against voltage (*open symbols*). The closed symbols represent time constants from single exponential fits to macroscopic currents (data kindly provided by Frank Horrigan). The single-channel data and the macroscopic data show similar kinetics at voltages above +200 mV. The differences between the two data sets at the lower voltages are most likely due to the relatively low open probability at those voltages—the small size of the ensemble averages prevented an accurate single exponential fit. (*B*) Po versus voltage curves. The symbols represent data from three different patches in zero calcium. The black curve is a Boltzmann curve generated from parameters reported in (Cui et al., 1997) for macroscopic *mSlo* currents in zero internal calcium. The single-channel data are shifted toward more positive voltages compared to the macroscopic current data. The dashed line is the macroscopic Boltzmann curve simply shifted to the right ~20 mV, and the gray line is the macroscopic curve scaled in the *y*-direction. Both manipulations to the curve representing the macroscopic data seem to fit the single-channel data.

ever, at these lower voltages, the ensemble averages were small, and the discrepancy between the single-channel and macroscopic current data may be due to difficulty in finding an accurate fit to the smaller ensemble average currents.

The probability that the single unliganded channel is open (P_o) increases with voltage (Fig. 3 *B*, *symbols*), as was seen in the macroscopic currents(Cui et al., 1997; Stefani et al., 1997). The single-channel data are from three different patches. The solid black curve in Fig. 3 *B* is derived from macroscopic *g–V* curves in zero calcium (Cui et al., 1997). The single-channel data seem to be shifted toward higher voltages relative to the macroscopic data. Scaling the macroscopic curve in the *y*-direction (*gray line*) fits the data, as would be expected from a difference in maximum open probability between the single-channel and the macroscopic current. Simply shifting the macroscopic curve by ~20 mV (*dashed line*) also fits the single-channel data. It is thus unclear whether the discrepancy between the macroscopic P_o–V and the single-channel data is due to a depression in the maximum open probability or to a shift in the channel's gating toward higher voltages. Variability in channel gating among different patches has been reported for both *mSlo* and *hSlo* (DiChiara and Reinhart, 1997; Stefani et al., 1997; Horrigan and Aldrich, 1999), and 20-mV differences in $V_{1/2}$ from patch to patch are not unusual. Determining whether the single-channel P_o continues to increase at higher voltages is impractical in our experiments, because the patches were not able to withstand such high voltages for the length of time necessary to attain the appropriate number of events. However, it is clear from Fig. 3 *B* that the probability of single-channel opening shows similar voltage dependence to the macroscopic currents.

Analysis of dwell-time distributions of the single-channel data can be used to determine the minimum number of conformational states that the channel can adopt, allowing a stringent test of the predicted two-state behavior of unliganded channels in the voltage-dependent MWC model of Fig. 1 *B*. The model predicts that such analysis should resolve only one component in the open dwell times and one component in the closed dwell times. Instead, the closed dwell time histograms were best fit with a sum of three exponentials, and the majority of the open dwell time histograms were best fit with a sum of two or three exponentials (Fig. 4). Additional exponential components were judged significant ($p < 0.5$) by the likelihood ratio test, (Rao, 1973; Horn and Lange, 1983), in which twice the difference in log likelihood of k versus $k - 1$ exponential components must be greater than 5.99, the χ^2 value for two degrees of freedom at the 0.05 confidence level. For our data, the value of the difference was usually three to five times larger than the required 5.99, indicating that the additional components are significant aspects of the dwell-time distributions. The multiple components found in the dwell-time distributions in zero calcium argue against the two-state voltage-dependent allosteric transition predicted by the MWC model (Fig. 1 *B*, *boxed region*) and indicate that the intrinsic voltage dependence of the single-channel molecule involves transitions between more than two conformational states. The presence of these multiple components requires that the voltage-dependent MWC model be expanded to allow for multiple unliganded open and closed states. These results also necessarily add several ligand-independent states to previously published models based on single-channel recordings obtained at moderate voltages and calcium concentrations (McManus and Magleby, 1991, 1988; Rothberg et al., 1997; Rothberg and Magleby, 1998). The model of Rothberg and Magleby (1999) suggests the presence of unliganded states, but they did not record from channels in the absence of calcium at any voltage. Our single-channel data in zero calcium are consistent with the presence of intermediate states inferred from macroscopic ionic and gating currents

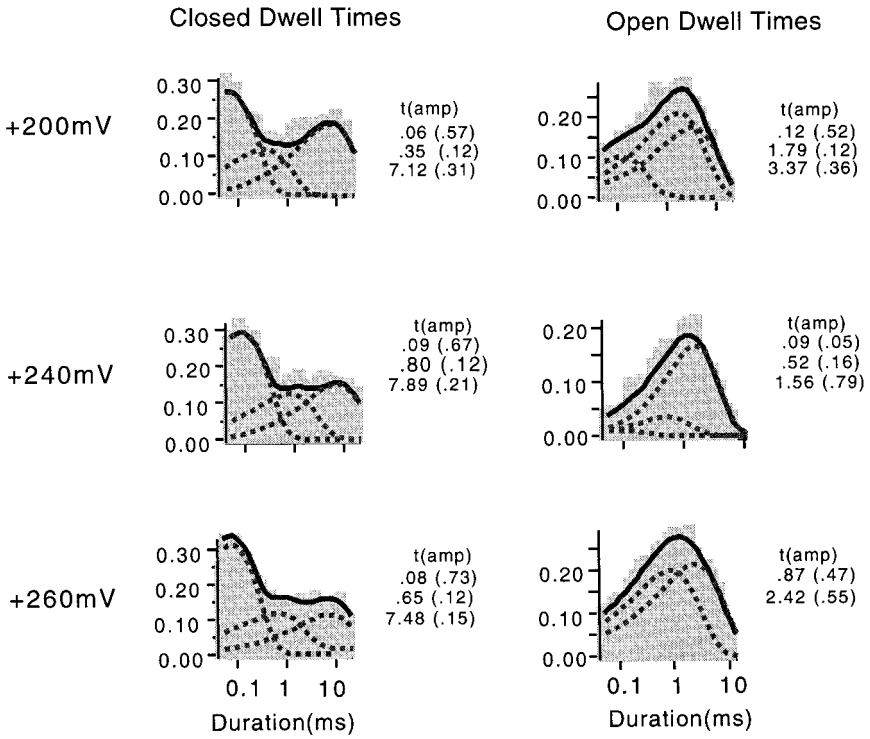

FIGURE 4 Dwell-time histograms reveal multiple components in both the closed and open dwell-time distributions. The exponential fits shown were directly fit to the data as described in Methods. These histograms represent data from a single patch recorded in zero internal calcium (5 mM EGTA). Two additional patches were analyzed across a similar voltage range. Open fit parameters: Patch 1: +160 mV: 0.33(0.11), 1.95(0.89); +200 mV: 0.42(0.17), 1.48(0.83); +240 mV: 1.95(1). Patch 2: +160: 0.15(0.32), 1.12(0.68); +200 mV: 0.08(0.03), 0.87(0.97). Closed fit parameters: Patch 1: +160 mV: 0.06(0.44), 0.44(0.13), 15.13(0.43); +200 mV: 0.08(0.52), 0.94(0.27), 8.22(0.22); +240 mV: 0.12(0.66), 5.34(0.34). Patch 2: +160 mV: 0.12(0.27), 22.63(0.73); +200 mV: 0.09(0.76), 5.52(0.24).

in the absence of calcium (Horrigan and Aldrich, 1999; Horrigan et al., 1999).

A characteristic feature of BK channel gating is fast "flicker" closings separating openings during a burst (Rothberg and Magleby, 1998). This bursting pattern of channel gating is present whether or not calcium is bound to the channel (see Fig. 2). The fast closed times within bursts must arise from conformational states that are distinct from those that give rise to the longer closed times between bursts, but the molecular basis of these short-lived flicker closed times is unclear. In the absence of calcium, the flickers show no voltage dependence (Fig. 5 *A*), and yet they represent a large proportion of the closed dwell times. Attributing a place for the flickers within kinetic mechanisms has proven difficult—even analyses of two-dimensional distributions composed of millions of events could not distinguish between a gating scheme that places the flickers within the activation pathway from a mechanism in which the channel must first open before it can access the flicker closed state (Rothberg and Magleby, 1998). The flickers are also not predicted by the voltage-dependent MWC model shown in Fig. 1 *B* (Cox et al., 1997). These fast closings could be unrelated to activation, and are perhaps a result of a fast voltage independent block by an unknown contaminant, or they could be due to voltage-independent transitions to conformational states outside the

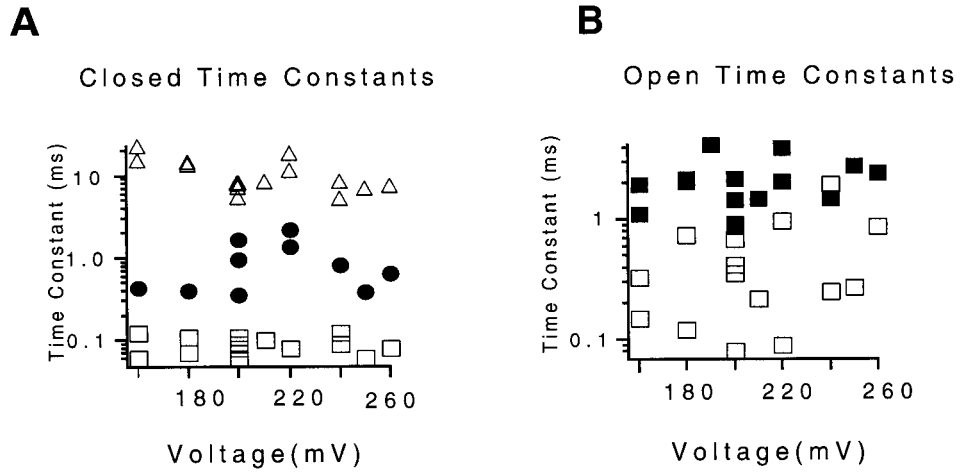

FIGURE 5 The components of the closed and open dwell-time distributions are not measurably sensitive to voltage. (*A*) and (*B*) show closed and open distribution time constants versus voltage from fits to dwell-time distributions, such as those shown in Fig. 4. The data are from three different patches. The different symbols represent different components of the distributions. None of the dwell-time components in either the open or the closed dwell-time distributions show any significant trends with voltage.

activation pathway (Hoshi et al., 1994; Schoppa and Sigworth, 1998).

If the flicker closings arise from mechanisms (block or otherwise) distinct from activation, their presence may mask a bursting behavior that is consistent with the two-state behavior predicted by the MWC model (Cox et al., 1997). We tested the two-state MWC prediction of the relationship between mean dwell times and ensemble average kinetics.

The model (Fig. 1 *B*) predicts that, in zero calcium, the single exponential kinetics of the ensemble averages should be related to the mean open and mean closed time in the following way:

$$\tau_{ens}^{-1} = (\text{mean open time})^{-1} + (\text{mean closed time})^{-1}.$$

Figure 6 *A* displays the mean open and closed times against voltage for three different patches. In Fig. 6 *B*, the filled squares represent τ_{ens}^{-1} and the circles represent the right side of the above expression: [(mean open time)$^{-1}$ + (mean closed time)$^{-1}$], both plotted against voltage. Figure 6 *B* shows that the above expression does not hold for our data. However, if the flicker closed times are effectively removed with the application of a burst criterion, then the same analysis using mean burst and mean interburst times (*triangles*) yields time constants that closely resemble the time constants of ensemble average activation, as predicted by the voltage-dependent MWC model. This analysis supports the idea that the burst and interburst durations determine the macroscopic kinetics and are consistent with a two-state MWC gating mechanism with the flicker closed state not a part of the activation process. However, as shown in the following analysis, the burst and interburst duration histograms are inconsistent with an MWC mechanism consisting of only a single burst and a single interburst state.

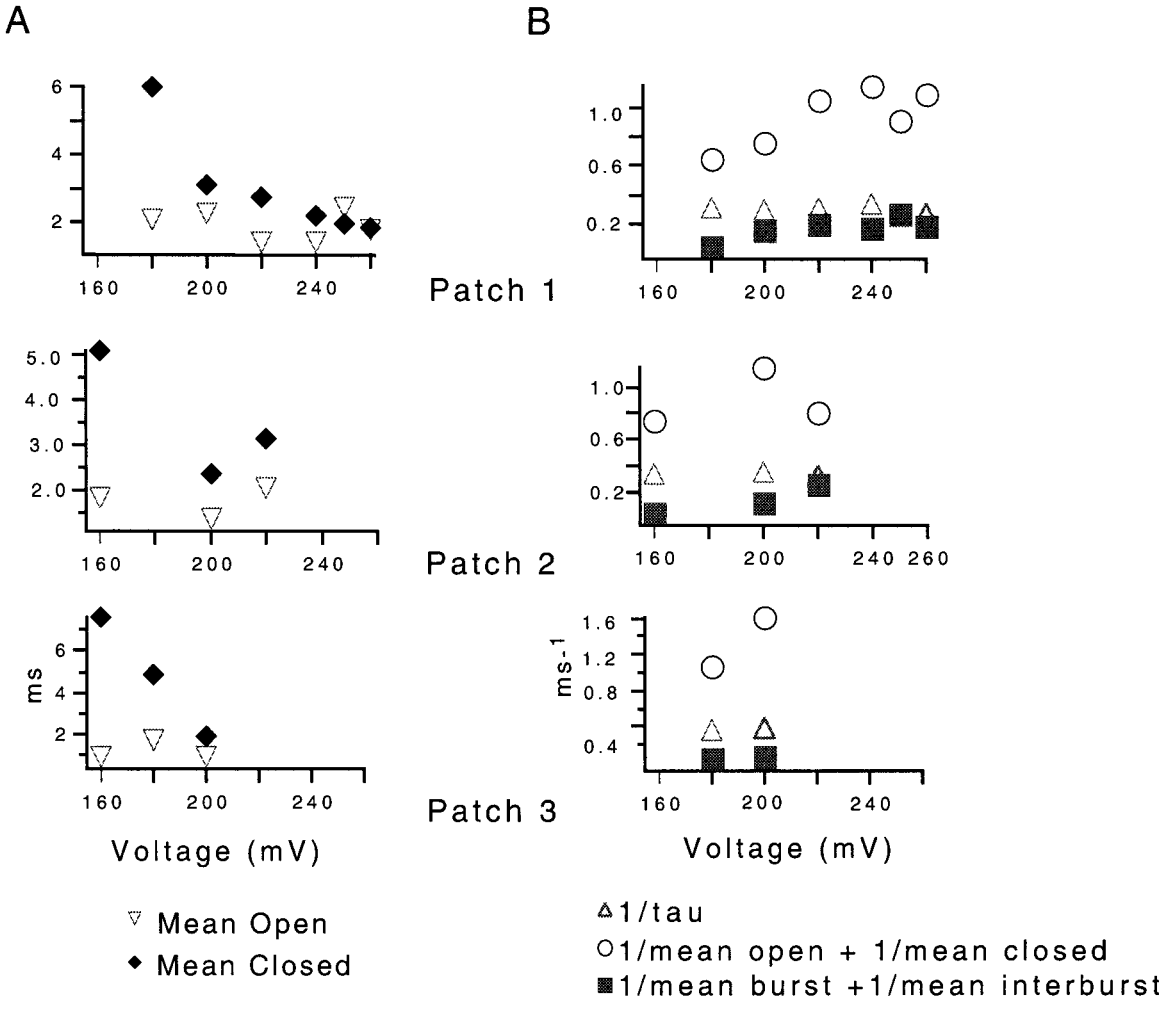

FIGURE 6 The voltage-dependent MWC model reported by Cui et al. (1997) predicts a specific relation between the single exponential kinetics of ensemble averages and the mean open and closed dwell times (see text). (*A*) Mean open and closed dwell times from three different patches. (*B*) Plots of the reciprocal time constant of fits to ensemble averages (*open triangle*) against voltage. Although these time constants do not correlate with the reciprocal of the mean open time plus the reciprocal of the mean closed time (*open circles*), as predicted by the voltage-dependent MWC model, the ensemble average time constants do correlate to the reciprocals of the mean burst + mean interburst dwell times.

Examination of the burst and interburst dwell times shows that, even when the flicker closed state is eliminated by application of the burst criterion, multiple components still remain in the burst and interburst distributions. Burst time distributions are best fit by the sum of at least two exponentials, and the interburst distributions are best fit by either one or two exponentials (Fig. 7). A mechanism that places flicker closed state (C_f) outside the activation pathway,

$$C \underset{\alpha}{\overset{\beta}{\leftrightarrow}} O \underset{k_{-b}}{\overset{k_{+b}}{\longleftrightarrow}} C_f$$

(Scheme 1)

could conceivably account for the double exponential distribution of the burst dwell-time histograms (see Colquhoun and Hawkes, 1995). During a burst, the channel travels back and forth between two states, open and the flicker closed, until the burst ends when the channel enters the longer-lived closed state. The sequential scheme pictured above could thus lead to the double exponential burst dwell-time distribution, and the deviations from the two-state predictions of the voltage-dependent MWC model would only be a result of the flicker closed state. Alternatively, the double exponential burst distribution could indicate a gating mechanism in which the channel can adopt more than one open-state conformation, which would be a serious deviation from the two-state predictions of the model.

To distinguish between these possibilities, we calculated the expected burst time distribution for the three-state bursting mechanism pictured in Scheme I. Such a mechanism predicts a double exponential burst duration distribution of the form

$$f(t) = a_1\lambda_1 e^{-\lambda_1 t} + a_2\lambda_2 e^{-\lambda_2 t}.$$

λ_1 and λ_2 can be determined by solving the quadratic equation

$$\lambda^2 + b\lambda + c = 0,$$

where $-b = \alpha + k_{+b} + k_{-b}$ and $c = \alpha k_{-b}$

All the parameters of this distribution can be determined from our data (see (Colquhoun and Hawkes, 1995)).

We calculated $-b$ from the following two expressions:

$$\text{mean open time} = (k_{+b} + \alpha)^{-1}$$

$$\text{mean flicker closed time} = 1/k_{-b}.$$

To determine c, we calculated α from the expression

$$\text{mean number of openings per burst} = 1 + \beta/\alpha,$$

where β is equal to the reciprocal of the mean interburst duration.

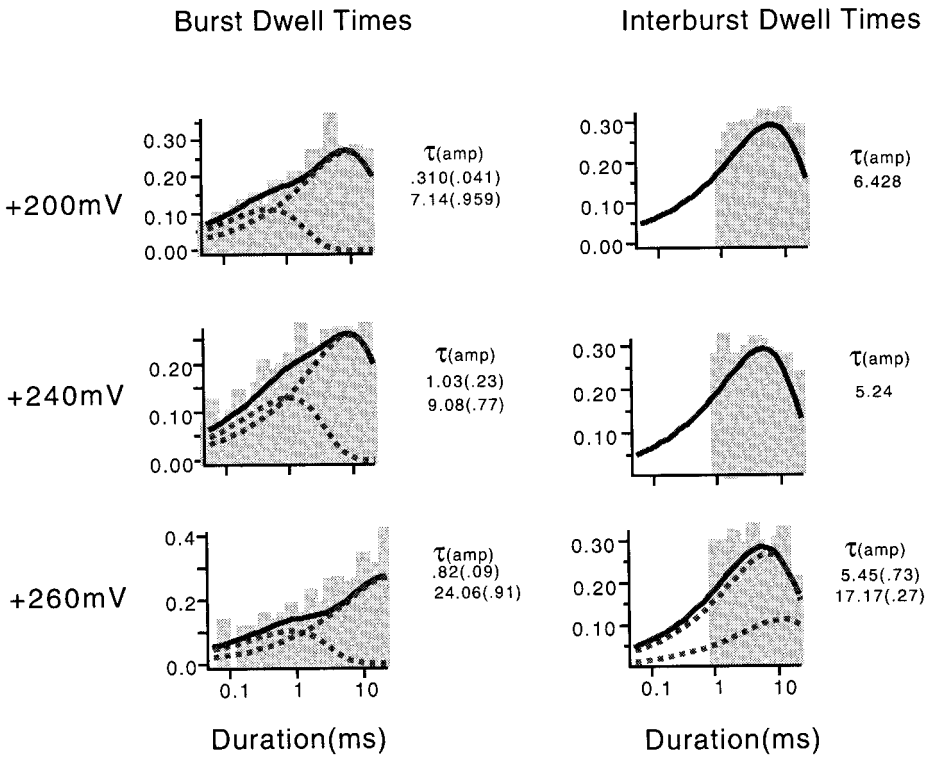

FIGURE 7 Multiple components remain in the burst and interburst dwell-time distributions. Burst and interburst dwell times are best fit with either one or two exponentials, indicating that the channel is able to adopt multiple conformational states. Two additional patches were analyzed across a similar voltage range. Burst fit parameters: Patch 1: +160 mV: 4.35(1); +200 mV: 0.10(0.08), 3.92(0.60), 12.01(0.32); +240 mV: 7.06(1). Patch 2: +160 mV: 1.33(0.80), 3.34(0.20); +200 mV: 4.37(1). Interburst fit parameters: Patch 1: +160 mV: 11.24(0.45), 24.85(0.55); +200 mV: 6.01(0.80), 18.33(0.20); +240 mV: 4.93(1). Patch 2: +160 mV: 9.81(1); +200 mV: 4.79(0.66), 21.56(0.34).

These calculations provided sufficient information to solve the following expressions for a_1 and a_2:

$$a_1 = \frac{\alpha(k_{-b} - \lambda_1)}{\lambda_1(\lambda_2 - \lambda_1)} \qquad a_2 = \frac{\alpha(\lambda_2 - k_{-b})}{\lambda_2(\lambda_2 - \lambda_1)}.$$

As Table 1 shows, the predicted burst dwell-time distributions would show an essentially single-exponential behavior, because the shorter time constant has such a low relative amplitude. In contrast, fits to the burst dwell-time distributions from our data reveal two well resolved exponential components with significant relative amplitudes. This analysis suggests that the two components of the burst dwell-time distributions cannot be accounted for by the flicker closings (Scheme I) and most likely represent distinct open conformational states (or groups of conformational states). Clearly, the flickers are not the sole cause of the complexity of channel gating in zero calcium. The simplest interpretation of these data is that the voltage-dependent step in channel activation is not fully concerted, as required by the model in Fig. 1 *B*, but that the channel is able to open even when only a subset of the subunits have voltage sensors in the active conformation (Horrigan et al., 1999; Horrigan and Aldrich, 1999).

If voltage is able to drive the channel to open with only a subset of its voltage sensors active, then a reasonable prediction is that the dwell time in these intermediate conformations will show a dependence on voltage. However, Fig. 5, *A* and *B* shows that the time constants of both the closed dwell-time distributions and the open dwell-time distributions show no significant change with voltage. These data suggest that, even an 80-mV change in membrane voltage is not enough to influence dwell time in the various open and closed conformational states that the channel is able to adopt. This apparent lack of voltage dependence may again be a reflection of the dominant effects of the flicker closed states. Because the flicker closed-time constants show no voltage dependence (Fig. 5 *A*), their dominance in the records could mask the voltage dependence of the other transitions (~80% of closings are to the flicker closed state, and ~93% of the openings are interrupted by flicker closings). We analyzed the burst dwell times to avoid the obscuring effects of the flicker closed states. As voltage increases, the longer component of the burst duration distribution increases (Fig. 8 *A*), as does its frequency within the dwell-time histogram (Fig. 8 *B*). These data suggest that the transitions from the open states to the longer-lived closed states are sensitive to changes in membrane voltage, and that this voltage sensitivity can be masked by the obscuring effects of the flicker closed states.

TABLE 1 Predicted and actual burst dwell-time distribution time constants

Voltage (mV)	Predicted τ(amp)	Actual τ(amp)
+200	0.089 ms (0.0002)	0.310 ms (0.041)
	15.53 ms (0.9998)	7.14 ms (0.959)
+240	0.102 ms (0.0003)	1.03 ms (0.23)
	21.29 ms (0.9997)	9.08 ms (0.77)
+260	0.105 ms (0.00023)	0.82 ms (0.09)
	26.6 ms (0.99977)	24.06 ms (0.91)

The voltage-dependent MWC model described by Cox et al. (1997) requires that the channel open with a concerted movement of all four subunits from the resting to the activated conformation. However, studies of *mSlo* gating currents (Horrigan and Aldrich, 1999) suggest that the channel can open even if all four voltage sensors have not moved to the activated conformation. Our single-channel data are consistent with this idea, with the multiple exponential components in the dwell-time distributions representing states or combinations of states with zero, one, two, three, or all four of the subunits in the activated conformation. For example, a channel with only one voltage sensor activated would presumably have a shorter open time than one with two or three active voltage sensors.

Because the dwell-time histograms showed multiple open and closed states, it is possible that the channels occupied these distinct states progressively as the probability of being open relaxed toward its equilibrium value during the voltage step. One advantage of studying single-channel gating using voltage steps rather than with steady-state recordings is that we can determine if the mechanism governing *mSlo* gating requires that the channel progress linearly through a specific order of states. Preferential occupancy of particular open or closed states earlier or later during the voltage pulse would indicate a preferred pathway of activation. For example, clusters of shorter open times toward the beginning of the sweep and longer open times at the end of the sweep would suggest a sequential mechanism in which the channel must pass through the shorter-lived open state before it can enter the longer-lived open state.

Plots of dwell time versus latency show no obvious trends in the open and closed and burst and interburst durations (Fig. 9). Because the channel is able to adopt multiple open and closed conformations (Figs. 4 and 7), the plots of dwell time versus latency in Fig. 8 show that there is no discernible preferred order to the way the channel adopts these multiple conformational states. Therefore, there must be many pathways between the different open and closed states to allow for the random distribution seen in the dwell times versus latency plots in Fig. 9. These results suggest that, even in the absence of calcium, the channel's kinetic mechanism is a branched pathway rather than a more linear mechanism with a preferred pathway of activation (such as the KNF scheme pictured in Fig. 1 *A*). A branched mechanism, such as the one proposed by Horrigan et al. (1999), can explain the random distribution of dwell times all along the duration of the sweep.

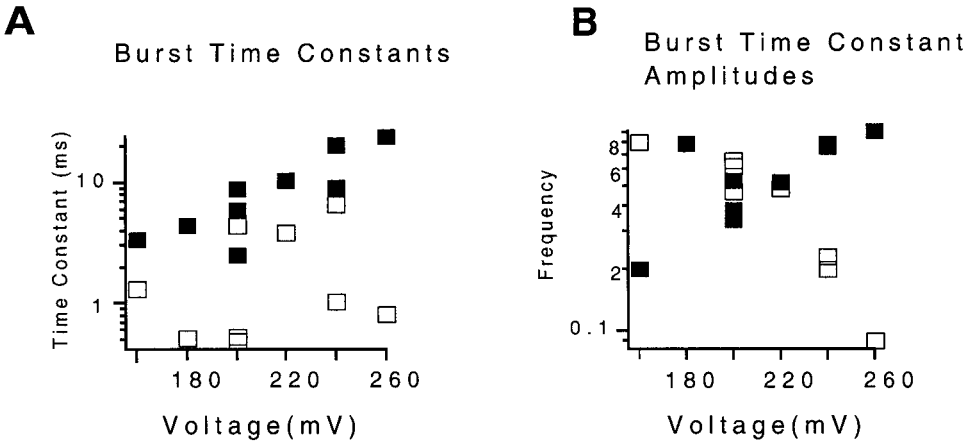

FIGURE 8 Although the components of the closed and open dwell-time distributions are not measurably sensitive to voltage (see Fig. 5), the components of the burst dwell-time distributions do change with voltage. (*A*) The longer time constant (*closed squares*) from fits to burst dwell-time distributions does increase in magnitude with voltage, suggesting that the channel spends more time in the burst state at higher voltages. (*B*) The relative amplitude of the longer burst-time constant (*closed square*) also increases with voltage, whereas the shorter time constant decreases. These data suggest that the channel is more likely to adopt the conformational state(s) represented by the longer time constant at increasing voltages.

DISCUSSION

The large conductance and stringent potassium selectivity of BK channels have made them a popular target of biophysical scrutiny. In particular, there have been many detailed single-channel analyses of BK gating behavior. These sophisticated studies yielded complicated kinetic mechanisms and quantitative estimates of the rate constants that govern transitions among the channel's various open and closed states. This work provided a detailed level of understanding of channel behavior under the specific conditions studied (moderate voltage, moderate-to-high intracellular calcium), but did not provide information on the gating of single unliganded channels. Macroscopic *mSlo* currents can be nearly maximally activated without binding calcium (Cui et al., 1997; Horrigan et al., 1999). One question we wished to answer in this paper was whether the complicated kinetic mechanisms seen in previous single-molecule studies of BK channels were solely a result of calcium's effects on the channel, or whether the channel has an intrinsically complex voltage-dependent mechanism. With the stringent conditions necessary to make recordings from single unliganded *mSlo* channels, it is impractical to obtain the number of events necessary to isolate the rate constants governing all transitions between conformational states, a goal that is perhaps more approachable in studies of liganded single BK channels. We have shown with a relatively simple analysis that the intrinsic voltage sensitivity of this channel is indeed complex even when no calcium is bound to the channel protein. Dwell-time distributions clearly show that the unliganded channel is able to adopt multiple open and closed states. Multiple conformational states can still be isolated when the flicker closed states are eliminated from the dwell-time analysis. We have also found that the transitions from the open states to the longer lived nonflicker closed states are sensitive to voltage. Our results suggest that any model of BK channel behavior will not be complete without an understanding of how the effects of calcium modify an intrinsically complex voltage-dependent mechanism.

Although most previous single-channel studies of BK channels did not account for unliganded openings, such spontaneous openings have been reported. Pallotta (1985) showed that, if rat skeletal muscle is treated with the protein-modifying reagent *N*-bromoacetamide, BK channel activity is no longer sensitive to intracellular calcium, although sensitivity to membrane voltage remains. The *N*-bromoacetamide-treated channels behaved similarly to untreated channels in zero calcium. Pallotta found that the channels had relatively simple kinetics and a low probability of opening, even at the highest voltages studied ($\sim$0.1 open probability at $+80$ mV).

Spontaneous openings have also been investigated in other ligand-gated channels. For example, cyclic nucleotide-gated channels are able to open spontaneously with low probability in the absence of any ligands (Picones and Korenbrot, 1995; Ruiz and Karpen, 1997; Tibbs et al., 1997). Liu et al. (1998) have further supported the concept of an intrinsic ligand-independent gating mechanism in cyclic nucleotide-gated channels by showing that the equilibrium between the unliganded closed and open state is not altered by mutating the ligand-binding site. Acetylcholine receptors are also able to spontaneously open in the absence of ligand (Jackson, 1984). Jackson was able to determine the steps of channel gating that respond to the binding of a ligand by comparing the behavior of the unliganded single channel to that of the liganded channel (Jackson, 1984). Other studies of unliganded acetylcholine receptors have

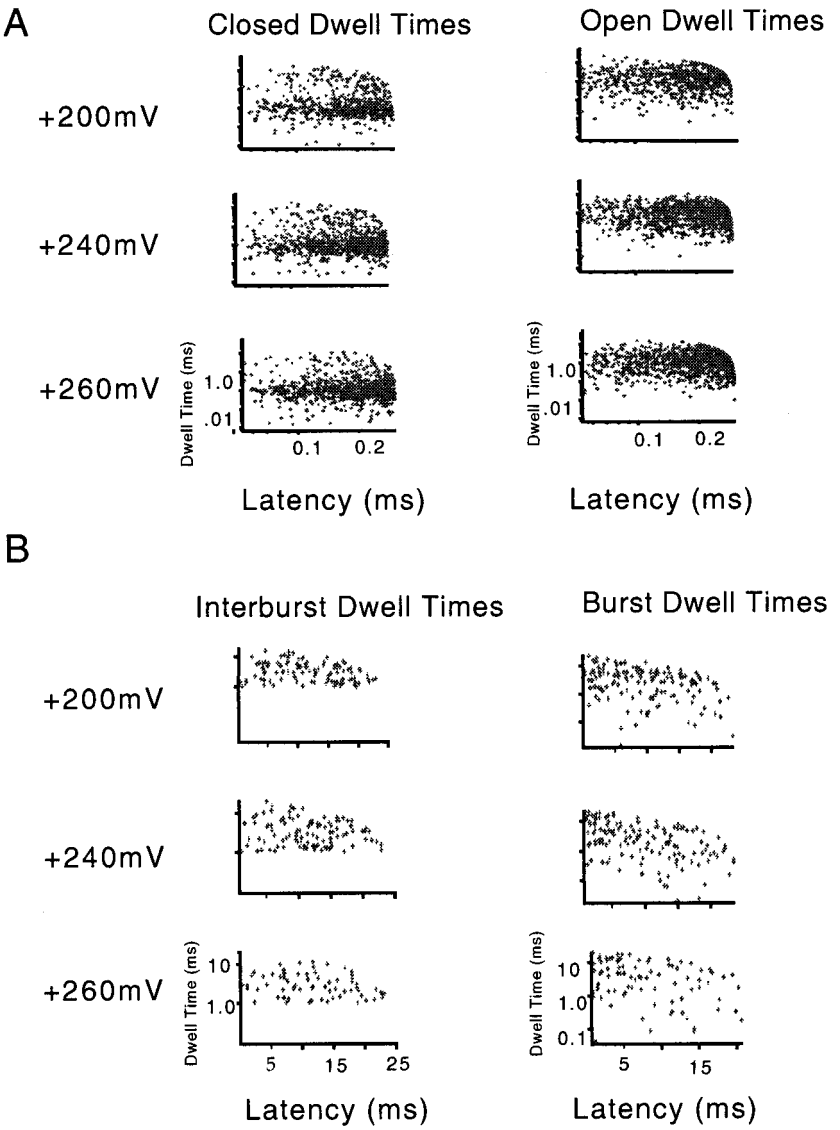

FIGURE 9 Dwell time versus latency plots reveal no significant trends in the dwell times throughout the duration of a voltage step. The data shown are from a single patch, and are representative of three patches. (*A*) Closed and open dwell time versus latency plots. The *y*-axes are on a logarithmic scale. (*B*) Interburst and burst dwell time versus latency plots. Burst criteria was 1 ms. The *y*-axes are on a logarithmic scale.

shown that, when the γ and ϵ subunits are removed, the receptor opens spontaneously at a high probability (Jackson et al., 1990), suggesting that these subunits influence gating by inhibiting spontaneous openings. Studies of unliganded channels have thus revealed details of gating mechanisms that could not have been obtained by studying only the behavior of their ligand-bound forms.

Rothberg and Magleby (1999) invoke a 50-state two-tiered kinetic mechanism to explain the single-channel behavior of the rat skeletal BK channel across a range of calcium concentrations. The fully liganded channel (calcium concentrations = 100 μM) occupies the extreme end of this kinetic mechanism, with five closed states and five open states. Because Rothberg and Magleby did not change the membrane voltage in that study, their results represent a flip side to our results here—a channel at constant voltage across a range of calcium concentration, whereas we are studying an unliganded channel across a range of voltages. It is interesting to note that, at both extremes, the unliganded channel and the fully liganded channel, the protein seems to have a complicated kinetic mechanism with multiple open and closed conformations.

Our results in zero calcium and the Rothberg and Magleby results at high calcium indicate that the mechanism proposed by Cox et al. (1997—also see Fig. 1 *B*) is too simple to explain BK-channel gating (as acknowledged by Cox et al., 1997). The model proposed by Cox et al. predicts that, at the two extremes of calcium binding, either completely unliganded or fully liganded, the channel's gating mechanism consists of a single concerted transition between two states, open and closed. The multiple kinetic states that Rothberg and Magleby report for the fully liganded channel and the multiple kinetic states that we see in zero calcium argue against a concerted two-state mechanism even under

these extreme conditions. Both studies suggest that the model proposed by Cox et al., and previous models that did not account for ligand-independent gating, must be expanded to account for the complicated kinetic mechanism of both the unliganded and the fully liganded channel.

Horrigan et al. (1999) have proposed a ten-state mechanism to describe *mSlo* gating in zero calcium. Single-channel records simulated from the Horrigan et al. model display kinetics that resemble the burst kinetics of single *mSlo* channels. However, like so many other models proposed to explain BK-channel gating, the Horrigan et al. model does not account for the flicker closed states, although other aspects of channel gating, such as voltage dependence and multiple open and closed conformational states, are well described by the model. Our single-channel data thus do not imply any greater complexity than what is described in the Horrigan et al. model, other than the presence of the flicker closed states.

The ten-state voltage-dependent mechanism described by Horrigan et al. suggests that the channel is able to open even if not all four voltage sensors have moved to the activated conformation. One interpretation of our single-channel results is that the multiple components we see in the open and closed dwell times of the channel in zero calcium represent states of the channel in which only a subset of the voltage sensors are in the activated conformation.

We gratefully acknowledge D. Perkins and D. Cox for development of the ScanApp analysis program, F. Horrigan for the donation of macroscopic current data and helpful comments on the manuscript, and E. Ogielska and D. Cox for helpful comments on the manuscript.

This work was supported by a National Institutes of Mental Health Silvio Conte Center for Neuroscience Research grant (MH 48108). R.W.A. is an investigator with the Howard Hughes Medical Institute. G.T. was supported by a fellowship from the National Science Foundation.

REFERENCES

Blatz, A. L., and K. L. Magleby. 1983. Single voltage-dependent chloride-selective channels of large conductance in cultured rat muscle. *Biophys. J.* 43:237–241.

Blatz, A., and K. Magleby. 1986. Correcting single channel data for missed events. *Biophy, J.* 49:967–980.

Brehm, P. R., R. Kullberg, and F. Moody-Corbett. 1984. Properties of non-junctional acetylcholine receptor channel in innervated muscle of *Xenopus laevis*. *J. Physiol.* 350:631–648.

Changeux, J. P., and S. J. Edelstein. 1998. Allosteric receptors after 30 years. *Neuron.* 21:959–980.

Colquhoun, D., and A. Hawkes. 1995. Stochastic interpretation of mechanism. *In* Single Channel Recording, B. Sakmann and E. Neher, editors. Plenum Press, New York. 397–480.

Colquhoun, D., and B. Sakmann. 1985. Fast events in single channel currents activated by acetylcholine and its analogues at the frog muscle end-plate. *J. Physiol.* 369:501–557.

Colquhoun, D., and F. J. Sigworth. 1995. Fitting and statistical analysis of single channel records. *In* Single-Channel Recording, B. Sakmann and E. Neher, editors, Plenum Press, New York. 483–585.

Cox, D. H., J. Cui, and R. W. Aldrich. 1997. Allosteric gating of a large conductance Ca-activated K+ channel. *J. Gen. Physiol.* 110:257–281.

Cui, J., D. H. Cox, and R. W. Aldrich. 1997. Intrinsic voltage dependence and Ca^{2+} regulation of *mSlo* large conductance Ca-activated K+ channels. *J. Gen. Physiol.* 109:647–673.

Diaz, F., M. Wallner, E. Stefani, L. Toro, and R. Latorre. 1996. Interaction of internal Ba^{2+} with a cloned Ca(2+)-dependent K+ (*hSlo*) channel from smooth muscle. *J. Gen. Physiol.* 107:399–407.

DiChiara, T. J., and P. H. Reinhart. 1997. Redox modulation of *hSlo* Ca^{2+}-activated K^+ channels. *J. Neurosci.* 17:4942–4955.

Edelstein, S. J., and J. P. Changeux. 1996. Allosteric proteins after thirty years: the binding and state functions of the neuronal alpha 7 nicotinic acetylcholine receptors. *Experientia.* 52:1083–1090.

Edelstein, S. J., and J. P. Changeux. 1998. Allosteric transitions of the acetylcholine receptor. *Adv. Protein Chem.* 51:121–184.

Fersht, A. 1985. Enzyme Structure and Mechanism, 2nd ed. W. H. Freeman and Co., New York.

Horn, R., and K. Lange. 1983. Estimating kinetic constants from single channel data. *Biophys. J.* 43:207–223.

Horrigan, F. T., J. Cui, and R. W. Aldrich. 1999. Allosteric voltage-gating of potassium channels. I. *mSlo* ionic currents in the absence of calcium. *J. Gen. Physiol.* 114:277–304.

Horrigan, F. T., R. W. and Aldrich. 1999. Allosteric voltage-gating of potassium channels. II. *mSlo* channel gating charge movement in the absence of calcium. *J. Gen. Physiol.* 114:305–336.

Hoshi, T., W. Zagotta, and R. Aldrich. 1994. *Shaker* potassium channel gating. I. Transitions near the open state. *J. Gen. Physiol.* 103:249–278.

Jackson, M. B. 1984. Spontaneous openings of the acetylcholine receptor channel. *PNAS.* 81:3901–3904.

Jackson, M. B., K. Imoto, M. Mishina, T. Konno, S. Numa, and B. Sakmann. 1990. Spontaneous and agonist-induced openings of an acetylcholine receptor channel composed of bovine muscle alpha-, beta- and delta-subunits. *Pflugers Arch.* 417:129–135.

Koshland, D. E., Jr., G. Nemethy, and D. Filmer. 1966. Comparison of experimental binding data and theoretical models in proteins containing subunits. *Biochemistry.* 5:365–385.

Liu, D. T., G. R. Tibbs, P. Paoletti, and S. A. Siegelbaum. 1998. Constraining ligand-binding site stoichiometry suggests that a cyclic nucleotide-gated channel is composed of two functional dimers. *Neuron.* 21:235–248.

McManus, O. B., and K. L. Magleby. 1988. Kinetic states and modes of single large-conductance calcium-activated potassium channels in cultured rat skeletal muscle. *J. Physiol.* 402:79–120.

McManus, O. B., and K. L. Magleby. 1989. Kinetic time constants independent of previous single-channel activity suggest Markov gating for a large conductance Ca-activated K channel. *J. Gen.Physiol.* 94: 1037–1070.

McManus, O. B., and K. L. Magleby. 1991. Accounting for the Ca(2+)-dependent kinetics of single large-conductance Ca(2+)-activated K+ channels in rat skeletal muscle. *J. Physiol.* 443:739–777.

Magleby, K. L., and B. S. Pallotta. 1983a. Calcium dependence of open and shut interval distributions from calcium-activated potassium channels in cultured rat muscle. *J. Physiol.* 344:585–604.

Magleby, K. L., and B. S. Pallotta. 1983b. Burst kinetics of single calcium-activated potassium channels in cultured rat muscle. *J. Physiol.* 344: 605–623.

Methfessel, C., and G. Boheim. 1982. The gating of single calcium-dependent potassium channels is described by an activation/blockade mechanism. *Biophys. Struct. Mech.* 9:35–60.

Moczydlowski, E., and R. Latorre. 1983. Gating kinetics of Ca^{2+}-activated K^+ channels from rat muscle incorporated into planar lipid bilayers. Evidence for two voltage-dependent Ca^{2+} binding reactions. *J. Gen. Physiol.* 82:511–542.

Monod, J., J. Wyman, and J.-P. Changeux. 1965. On the nature of allosteric transitions: a plausible model. *J. Mol. Biol.* 12:88–118.

Neyton, J. 1996. A Ba^{2+} chelator suppresses long shut events in fully activated high-conductance Ca(2+)-dependent K^+ channels. *Biophys. J.* 71:220–226.

Pallotta, B. S., K. L. Magleby, and J. N. Barrett. 1981. Single channel recordings of Ca^{2+}-activated K^+ currents in rat muscle cell culture. *Nature.* 293:471–474.

Pallotta, B. S. 1985. *N*-bromoacetamide removes a calcium dependent component of channel opening from calcium-activated potassium channels in rat skeletal muscle. *J. Gen. Physiol.* 86:601–611.

Pallotta, B. S., A. L. Blatz, and K. L. Magleby. 1992. Recording from calcium-activated potassium channels. *Meth. Enzymol.* 207:194–207.

Picones, A., and J. I. Korenbrot. 1995. Spontaneous, ligand-independent activity of the cGMP-gated ion channels in cone photoreceptors of fish. *J. Physiol.* 485:699–714.

Rao, C. R. 1973. Linear Statistical Inference and Its Applications. John Wiley, New York.

Rothberg, B. S., R. A. Bello, L. Song, and K. L. Magleby. 1996. High Ca^{2+} concentrations induce a low activity mode and reveal Ca2(+)-independent long shut intervals in BK channels from rat muscle. *J. Physiol.* 493:673–689.

Rothberg, B. S., R. A. Bello, and K. L. Magleby. 1997. Two-dimensional components and hidden dependencies provide insight into ion channel gating mechanisms. *Biophys. J.* 72:2524–2544.

Rothberg, B. S., and K. L. Magleby. 1998. Kinetic structure of large-conductance Ca^{2+}-activated K^+ channels suggests that the gating includes transitions through intermediate or secondary states. A mechanism for flickers. *J. Gen. Physiol.* 111:751–780.

Rothberg, B. S., and K. L. Magleby. 1999. Gating kinetics of single large-conductance Ca^{2+}-activated K^+ channels in high Ca^{2+} suggest a two-tiered allosteric gating mechanism. *J. Gen. Physiol.* 114:93–124.

Ruiz, M. L., and J. W. Karpen. 1997. Single cyclic nucleotide-gated channels locked in different ligand-bound states. *Nature.* 389:389–392.

Schoppa, N., and F. Sigworth. 1998. Activation of *shaker* potassium channels. I. Characterization of voltage-dependent transitions. *J. Gen. Physiol.* 111:271–294.

Silberberg, S. D., A. Lagrutta, J. P. Adelman, and K. L. Magleby. 1996. Wanderlust kinetics and variable Ca(2+)-sensitivity of *dSlo* [correction of *Drosophila*], a large conductance CA(2+)-activated K^+ channel, expressed in oocytes. Article originally printed in *Biophys. J.* 70: 2640–2651. [Corrected and republished with original paging as an erratum, *Biophys. J.* 71:2640–2651.]

Stefani, E., M. Ottolia, F. Noceti, R. Olcese, M. Wallner, R. Latorre, and L. Toro. 1997. Voltage-controlled gating in a large conductance Ca^{2+}-sensitive K^+ channel (*hSlo*). *Proc. Natl. Acad. Sci. USA.* 94: 5427–5431.

Tibbs, G. R., E. H. Goulding, and S. A. Siegelbaum. 1997. Allosteric activation and tuning of ligand efficacy in cyclic-nucleotide-gated channels. *Nature.* 386:612–615.